DOI:10.1111/j.1750-2659.2010.00147.x
www.influenzajournal.com

Original Article

Pandemic influenza A (H1N1) during winter influenza season in the southern hemisphere

Ying-Hen Hsieh

Department of Public Health and Center for Infectious Disease Epidemiology Research, China Medical University, Taichung, Taiwan.
Correspondence: Ying-Hen Hsieh, Department of Public Health and Center for Infectious Disease Epidemiology Research, China Medical University, 91 Hsueh-Shih Road, Taichung 40402, Taiwan. E-mail: hsieh@mail.cmu.edu.tw

Accepted 1 June 2010. Published Online 28 June 2010.

Background Countries in the southern hemisphere experienced sizable epidemics of pandemic influenza H1N1 in their winter season during May–August, 2009.

Methods We make use of the Richards model to fit the publicly available epidemic data (confirmed cases, hospitalizations, and deaths) of six southern hemisphere countries (Argentina, Brazil, Chile, Australia, New Zealand, and South Africa) to draw useful conclusions, in terms of its reproduction numbers and outbreak turning points, regarding the new pH1N1 virus in a typical winter influenza season.

Results The estimates for the reproduction numbers of these six countries range from a high of 1·53 (95% CI: 1·22, 1·84) for confirmed case data of Brazil to a low of 1·16 (1·09, 1·22) for pH1N1 hospitalizations in Australia. For each country, model fits using confirmed cases, hospitalizations, or deaths data always yield similar estimates for the reproduction number. Moreover, the turning points for these closely related outbreak indicators always follow the correct chronological order, i.e., case–hospitalization–death, whenever two or more of these three indicators are available.

Conclusions The results suggest that the winter pH1N1 outbreaks in the southern hemisphere were similar to the earlier spring and later winter outbreaks in North America in its severity and transmissibility, as indicated by the reproduction numbers. Therefore, the current strain has not become more severe or transmissible while circulating around the globe in 2009 as some experts had cautioned. The results will be useful for global preparedness planning of possible tertiary waves of pH1N1 infections in the fall/winter of 2010.

Keywords pandemic influenza, pH1N1, reproduction number, Richards model, southern hemisphere, turning point.

Please cite this paper as: Hsieh Ying-Hen. (2010) Pandemic influenza A (H1N1) during winter influenza season in the southern hemisphere. Influenza and Other Respiratory Viruses 4(4), 187–197.

Introduction

The pandemic influenza H1N1 2009 (pH1N1) was first identified by the Centers for Disease Control in two children in April.[1] As of 14 February 2010, worldwide more than 212 countries and overseas territories or communities have reported laboratory-confirmed cases of pandemic influenza H1N1 2009, including at least 15921 deaths.[2]

As predicted earlier by many experts (e.g., 3), the southern hemisphere also witnessed a sizable epidemic of pH1N1 in its winter season during May–August, with attack rates exceeding those in a typical influenza season in these countries. Moreover, it is important to monitor changes in antigenicity, severity, transmissibility, and antiviral resistance in the southern hemisphere to compare with those of the spring and winter outbreaks in the northern hemisphere. We construct simple mathematical models using the epidemiologic data for these southern hemisphere countries to draw timely and useful conclusions regarding the role played by the new pH1N1 strain under the setting of a typical winter influenza season.

Methods and materials

Data

We obtain the 2009 pH1N1 data for Argentina, Chile, and Brazil used in this study from the respective Ministries of Health of Argentina,[4] Chile,[5] and Brazil[6] websites. The New Zealand data were accessed from the Institute of Environmental Science and Research of New Zealand website.[7] The Australian data were obtained from Department of Health and Ageing website.[8] The South Africa data were accessed from the National Institute for Communicable Diseases (NICD) website.[9]

Methods

Richards[10] proposed the following model to study the growth of biologic populations:

$$C'(t) = rC(t)[1 - (\frac{C}{K})^a].$$

Here, the prime '' denotes the derivative or time rate of change and the time unit is in days or epidemiological weeks (or e-weeks that start on Sunday and end on Saturdays), depending on the time unit of the data used. $C(t)$ is the cumulative number of cases (confirmed, hospitalization, or death) at time unit (day or week) t, K is the 'maximum' case number or the final outbreak size over a single wave of outbreak, r is the per capita growth rate of the cumulative number of cases, while a is an exponent of deviation of the epidemiologic curve. The solution of Richards model can be explicitly given in terms of its model parameters and the initial value C(0) as $C(t) = K[1 + e^{-r(t-t_m)}]^{-1/a}$. The parameter t_m is related to the turning point t_i (defined as the time when the rate of case accumulation changes from increasing to decreasing or vice versa) of the epidemic by the simple formula $t_m = t_i + (\ln a)/r$, where ln denotes the natural logarithm function. By fitting cumulative case data of a particular outbreak, these four quantities, namely, the growth rate r, carrying capacity K, inflection point t_i, and exponent of deviation a of the model, can be obtained simultaneously using standard software such as MATLAB or SAS.

In this model formulation, the basic reproduction number R_0 is given by the formula $R_0 = \exp(rT)$, where T is the disease generation time (or generation interval) defined as the average time interval from one person being infected to the time when an infection by this infected individual occur.

The estimation of mean generation time could be difficult because it is often impractical to report observed generation time, and sophisticated statistical procedures have been developed to attain this goal (see e.g., [11,12]). Moreover, it has been shown mathematically[11] that, given the growth rate r, the expression $R_0 = \exp(rT)$ provides the upper bound of basic reproduction number regardless of the distribution of the generation interval that is being used.

In the case where there is little prior human immunity for the virus under consideration, the estimate for R_0 approximates the number of infections caused by an infectious individual entering an immunologically naïve population. Readers are referred to[13–15] for more technical details regarding the Richards model.

The basic premise of the Richards model is that the incidence curve of a single wave of infections consists of a single peak of high incidence, resulting in an S-shaped cumulative epidemic curve with a single turning point for the outbreak. The turning point t_i can be easily pinpointed by locating the inflection point of the cumulative case curve, i.e., the moment at which the trajectory begins to decline. This quantity in time has obvious epidemiologic importance, indicating either the beginning of a new wave of infections (i.e., moment of acceleration after deceleration) or the end of the current wave of infections (i.e., moment of deceleration after acceleration).

One of the advantages in using the Richards model for mathematical modeling is to fit the accumulative case number, which helps to smooth out the stochastic variations in epidemic curve owing to variations in data collection. When there are indeed two or more waves of infections, a variation of the S-shaped Richards model has been proposed,[14] which distinguishes between two types of turning points: one in the initial S curve that signifies the first turning point that ends initial exponential growth (or a downturn in case number) and a second type of turning point in the epidemic curve where the growth rate of the number of cumulative cases begin to increase again (or a upturn in case number), signifying the beginning of the next wave of infections. This variation of the Richards model provides a systematic method of determining whether an outbreak is 1-wave or multi-wave in nature, and is designed to isolate the main turning points from those peaks and valleys resulting from the data stochasticity. More details on the multi-wave Richards model can be found in,[14–16] where 2003 SARS incidence curves for the Great Toronto Area and Singapore are shown to contain two peaks (local maximum or turning point of the first type) and one valley (local minimum or turning point of second type). The readers are also referred to[14] for its application to 2-wave dengue outbreak in Taiwan in 2007.

We note that the estimates of R_0 should be valid for the new H1N1 strain, although discrepancy might exist because of prior immunity.[17] Moreover, no mass intervention measures (e.g., community-level isolation/quarantine/closure) were implemented at any time during the course of the outbreaks, although some measures were taken in each country with varying degrees of impact. To be conservative in our conclusions, we will henceforth denote the reproduction number obtained here as the *effective* reproduction number R of the outbreak in question.

Results

We fit the cumulative pandemic influenza A (H1N1) 2009 case data from various southern hemisphere countries described earlier to the Richards model and its multi-wave variants. The country-wise results of model parameter estimation, using least squares techniques, are detailed in the following text. For the purpose of computing R_0, we make use of the mean estimated generation interval (and its 95% CI) of T = 1·91 days (95% CI: 1·30–2·71) as given in,[18] which was estimated from early Mexico novel H1N1 data before April 30.

Argentina

The daily 2009 pH1N1 confirmed case, hospitalization [of all severe respiratory infections or sever respiratory infection (SRI)], and pH1N1 death data of Argentina[4] during May 19 to August 23 are fitted to the Richards model. The results of model parameter estimation for Argentina are given in Tables 1 and 2. Table 1 shows that the daily confirmed pH1N1 case data fit both 1-wave and 2-wave Richards models. Using the daily confirmed case data, the 1-wave model fit gives a turning point of June 26, while the 2-wave yields 3 turning points, one 'downturn' tuning point for each wave around June 1 and June 24, and an 'upturn' turning point on June 4 signifying the start of the second wave. For comparison, both the daily SRI hospitalization data (6/1–7/25) and daily pH1N1 death data (6/12–8/20) fit 1-wave Richards models (Table 2). The turning point using daily SRI hospitalization data is June 28, while the turning point for the daily H1N1 death data is July 1. For the purpose of comparison with the estimates for the final case number K for each wave of outbreak, we also provide the actual case numbers in the table legends.

The estimates for the reproduction number, using the daily confirmed pH1N1 case data, are $R = 1{\cdot}41$ (95% CI: 1·23, 1·60), and 1·84 (95% CI: 0·86, 2·82) and 1·34 (95% CI: 1·19, 1·48), respectively, for the 2-wave model. The corresponding estimates are $R = 1{\cdot}27$ (95% CI: 1·16, 1·38) and 1·28 (95% CI: 1·16, 1·39), respectively, using SRI hospitalization and pH1N1 death data. The graphs of the theoretical curves are shown in Figure 1A–D.

Chile

The weekly pH1N1 hospitalization data by onset week of e-week 20–33 (May 10 to August 15) and daily death data of June 1 to August 18 in Chile[6] fit 1-wave Richards model (Table 3 and Figure 1E–F). The turning point for weekly pH1N1 hospitalization data is e-week 26, whereas the turning point for the daily death data is July 11. The estimated reproduction numbers are 1·24 (95% CI: 1·14, 1·35) for weekly pH1N1 hospitalization data and 1·29 (95% CI: 1·17, 1·41) for the daily death data. Note that the confirmed pH1N1 case data for Chile did not converge for earlier Ministry of Health of Chile Pandemic Virus Report reported in July, most likely attributable to the transient state of data collection during earlier stages of the outbreak (e.g., changing case definitions and level of surveillance), and was not given in the Pandemic Influenza Report in August[5] and onward.

Brazil

The weekly pH1N1 confirmed case data by onset week of e-week 21–33 (May 17 to August 15) in Brazil[6] also fits both 1-wave and 2-wave Richards models (Table 4). The turning point for 1-wave model is e-week 31, while the two respective 'downturn' turning points for the two waves are e-week 26 and e-week 31. The estimated reproduction numbers are 1·53 (95% CI: 1·22, 1·84) for 1-wave model, and 1·66 (95% CI: 1·23, 2·09) and 1·39 (95% CI: 0·99, 1·79) for the respective two waves of the 2-wave model. The graph for model fit is given in Figure 1G.

Table 1. Estimation results using daily confirmed pH1N1 case data by onset date in Argentina with 1-wave and 2-wave Richards models. Turning point t_i denotes the number of days after the beginning of the wave of outbreak. The actual case number is 15104 for the whole period, 1159 for the first wave (5/19–6/4), and 14041 for the second wave (6/4–8/23)

Model	Time period	Turning point t_i (95% CI)	Growth rate r (95% CI)	Case number K (95% CI)	R (95% CI)
1-wave	5/19–8/23	37·11 (June 26) (35·65, 38·56)	0·18 (0·16, 0·20)	14736 (14651, 14822)	1·41 (1·23, 1·60)
2-wave	5/19–6/4	12·72 (June 1) (9·92, 15·52)	0·32 (0·07, 0·57)	1561 (991, 2131)	1·84 (0·86, 2·82)
	6/4–8/23	19·60 (June 24) (16·49, 22·71)	0·15 (0·14, 0·16)	13726 (13653, 13798)	1·34 (1·19, 1·48)

Table 2. Estimation results using daily sever respiratory infection (SRI) hospitalization data and pH1N1 death data in Argentina fitting with the 1-wave Richards model. Turning point t_i denotes the number of days after the beginning of the wave of outbreak. The actual hospitalization number is 5390 and number of deaths is 371

Data	Time Period	Turning point t_i (95% CI)	Growth rate r (95% CI)	Case number K (95% CI)	R (95% CI)
Hospitalization	6/1–7/25	26·42 (June 28) (15·98, 36·87)	0·12 (0·12, 0·13)	5520 (5459, 5581)	1·27 (1·16, 1·38)
Death	6/12–8/20	18·85 (July 1) (15·61, 22·09)	0·13 (0·13, 0·13)	372 (371, 373)	1·28 (1·16, 1·39)

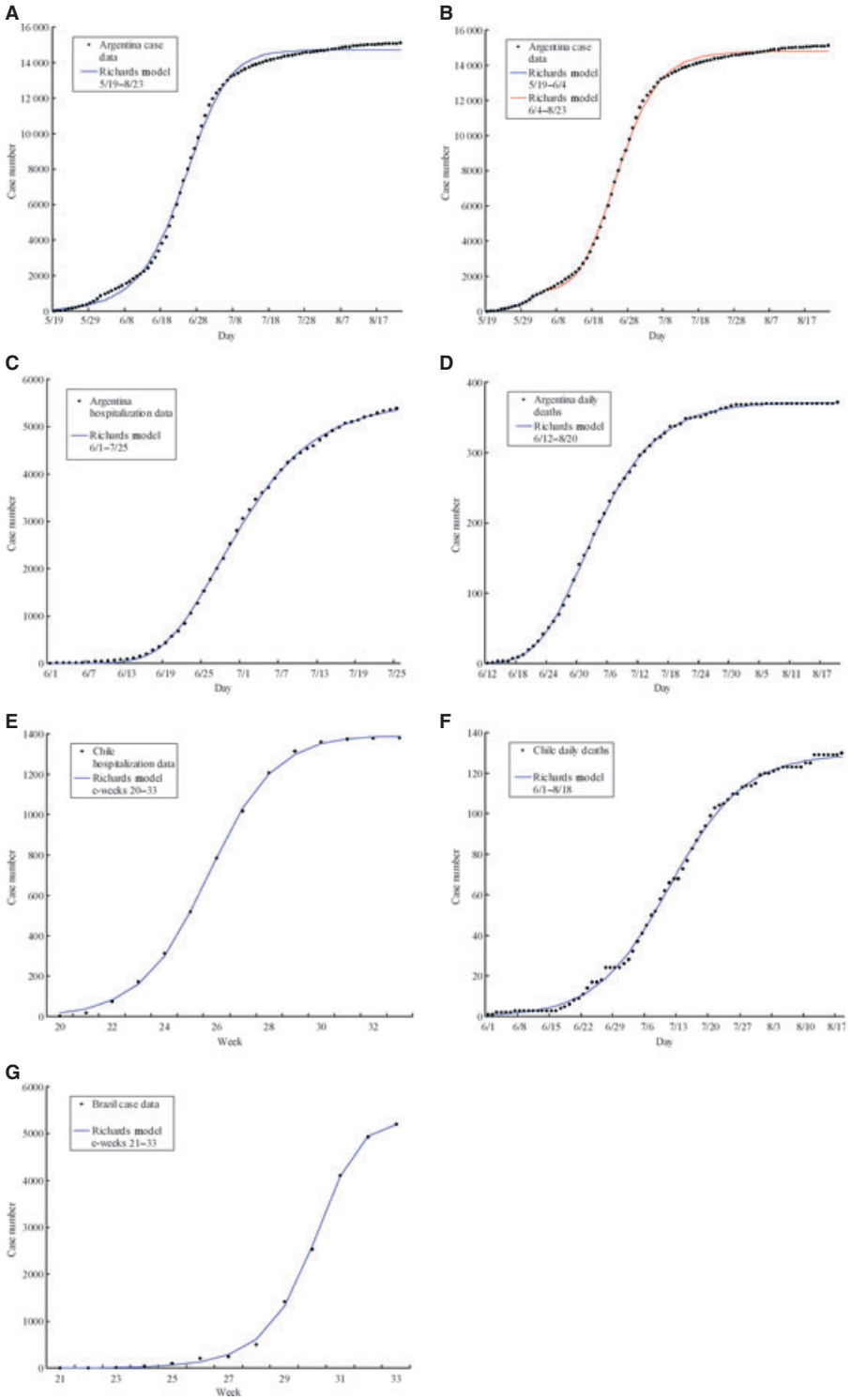

Figure 1. Theoretical curves obtained from Richards model and 2009 H1N1 cumulative data: (1A) 1-wave model using Argentina daily cumulative confirmed case data (5/19–8/23); (1B) 2-wave model using Argentina daily cumulative confirmed case data (5/19–8/23); (1C) 1-wave model using Argentina daily cumulative severe respiratory infections hospitalization data; (1D) 1-wave model using Argentina daily cumulative death data (6/13–8/20); (1E) 1-wave model using Chile weekly cumulative hospitalization case data by onset week of e-weeks 20–33 (May 10 to August 15); (1F) 1-wave model using Chile daily cumulative death data of June 1 to August 18; (1G) 1-wave Richards model using Brazil 2009 H1N1 daily cumulative confirmed case data of e-week 21–33 (May 17 to August 15).

New Zealand

We first note that the New Zealand data are given in calendar weeks ending on Sundays,[7] as opposed to e-weeks that end on Saturdays. The weekly pH1N1 confirmed case data by onset week of weeks ending on April 12–September 20 and weekly pH1N1 hospitalization data by hospitalization, onset, or report week of weeks ending on June 7–September 13 in New Zealand[7] fit 1-wave Richards models (Table 5 and Figure 2A–D). Moreover, the sentinel and non-sentinel surveillance data by reporting week of weeks ending on June 14–September 20 and May 3–September 20, respectively, also fit 1-wave Richards models. The turning point for the weekly pH1N1 confirmed case data is the week ending July 5 and for the hospitalization data is the succeeding week ending July 12, giving strong evidence that the turning point for the better had occurred by early July. The turning point for the sentinel and non-sentinel surveillance data are the weeks ending July 19 and July 12, respectively.

The estimated reproduction numbers are 1·22 (95% CI: 1·13, 1·31) for the weekly confirmed case data; 1·29 (95% CI: 1·16, 1·41) for weekly pH1N1 hospitalization data; 1·18 (95% CI: 1·10, 1·25) for the sentinel; and 1·22 (95% CI: 1·13, 1·31) for the non-sentinel surveillance data.

Australia

The weekly pH1N1 confirmed case and hospitalization data by onset week in Australia[8] fit the 1-wave Richards model (Table 6 and Figure 2E–F). The turning point for both the weekly pH1N1 confirmed case data and the hospitalization data is e-week 30, showing that the down turning point of case number had occurred by late July. The estimated reproduction numbers are 1·19 (95% CI: 1·11, 1·26) for the weekly confirmed case data; 1·16 (95% CI: 1·09, 1·22) for weekly pH1N1 hospitalization data.

South Africa

The weekly pH1N1 confirmed case data of weeks ending on July 5 to September 20 in South Africa[9] fit the 1-wave Richards model (Table 7 and Figure 2G). The turning point for the weekly pH1N1 confirmed case data is the week ending August 16. The estimated reproduction number is 1·22 (95% CI: 1·11, 1·33).

Sensitivity analysis

Several alternate estimates of the generation time T have been reported. Hence, we perform sensitivity analysis on R for Argentina and New Zealand data using estimates of T obtained from pH1N1 data in US: $T = (2{\cdot}6,\ 3{\cdot}2)$[19] and $T = 2{\cdot}5$[20]; in Netherlands: $T = 2{\cdot}7$ (SD = 1·1);[21] and in Japan: $T = 2{\cdot}83$ (Variance = 1·26) [Nishiura, personal communications]. The resulting estimates for R are given in Tables 8 and 9.

Conclusions and discussions

Reproduction number

The reproduction numbers obtained here are very similar, all of which are in agreement with the recent estimates for Mexico[18,22] and Canada (Tuite *et al.* unpub. manuscript and Hsieh *et al.* unpub. manuscript). The estimates for

Table 3. Estimation results using weekly pH1N1 hospitalization and daily death data in Chile with 1-wave Richards model. Turning point t_i denotes the number of days or weeks after the beginning of the wave of outbreak. The actual hospitalization number is 1381 and number of deaths is 130

Data	Time period	Turning point t_i (95% CI)	Growth rate r (95% CI)	Case number K (95% CI)	R (95% CI)
Hospitalization	e-weeks 20–33	5·70 (e-week 26) (5·13, 6·26)	0·80 (0·69, 0·90)	1394 (1375, 1413)	1·24 (1·14, 1·35)
Death	6/1–8/18	39·90 (July 11) (37·56, 42·23)	0·12 (0·11, 0·13)	129 (128, 131)	1·29 (1·17, 1·41)

Table 4. Estimation results using weekly pH1N1 confirmed case data by onset week in Brazil with 1-wave and 2-wave Richards models. Turning point t_i denotes the number of weeks after the beginning of the wave of outbreak. The actual case number is 5206 for the whole period

Model	E-weeks	Turning point t_i (95% CI)	Growth rate r (95% CI)	Case number K (95% CI)	R (95% CI)
Estimate 1	21–33	9·30 (e-week 31) (8·95, 9·65)	1·56 (1·08, 2·03)	5281 (5090, 5471)	1·53 (1·22, 1·84)
Estimate 2	21–27	4·36 (e-week 26) (3·95, 4·78)	1·85 (1·18, 2·53)	264 (249, 280)	1·66 (1·23, 2·09)
	27–33	3·10 (e-week 31) (1·09, 5·11)	1·20 (0·23, 2·17)	5183 (4542, 5823)	1·39 (0·99, 1·79)

Table 5. Estimation results using weekly pH1N1 confirmed and hospitalized cases by earliest reporting week; sentinel and non-sentinel surveillance case data by reporting week in New Zealand with the 1-wave Richards model. Turning point t_i denotes the number of weeks after the beginning of the wave of outbreak. The actual case number is 3200 confirmed cases, 973 for the hospitalizations, 622 for sentinel surveillance, and 4281 for non-sentinel surveillance

Data	Time period	Turning point t_i (95% CI)	Growth rate r (95% CI)	Case number K (95% CI)	R (95% CI)
Confirmed case	Weeks ending 4/12–9/20	11·88 (Week ending on 7/5) (11·13, 12·63)	0·72 (0·65, 0·80)	3184 (3157, 3210)	1·22 (1·13, 1·31)
Hospitalization	Weeks ending 6/7–9/13	4·15 (Week ending on 7/12) (3·54, 4·77)	0·92 (0·81, 1·03)	967 (958, 975)	1·29 (1·16, 1·41)
Sentinel surveillance	Weeks ending 6/14–9/20	10·22 (Week ending on 7/19) (9·56, 10·89)	0·60 (0·54, 0·66)	625 (618, 631)	1·18 (1·10, 1·25)
Non-sentinel surveillance	Weeks ending 5/3–9/20	20·17 (Week ending on 7/12) (19·45, 20·88)	0·73 (0·64, 0·82)	4253 (4209, 4297)	1·22 (1·13, 1·31)

Chile, Brazil, Australia, New Zealand, and South Africa are in close agreement with estimates by the WHO informal mathematical modeling network for 2009 influenza pandemic,[23] as well as numerous estimates for spring/summer outbreaks of other countries in literature (see Table 2, 23). The estimates for R in Argentina and New Zealand obtained by using different estimates of generation interval (T) for 2009 pH1N1 in the literature are also in close agreement (Tables 8 and 9). The results indicate that higher values of T will raise all the estimates for R, as can be expected from the formula for R given earlier. For the Argentina hospitalization data with $T = 1{\cdot}91$[18], $R = 1{\cdot}27$ is obtained; whereas using a T value of around $2{\cdot}7$[21] we have $R = 1{\cdot}40$ (see Table 8B). Both estimates are within reasonable range. However, the discrepancy becomes larger for larger values of R (see next to last row, Table 8A), thus indicating the dependence of R on accurate estimate of T. The corresponding estimates for other countries are similar and hence are omitted for brevity.

The estimates for New Zealand are substantially lower than the range of 1·49–2·55 for reproduction number obtained in,[24] using the case data of 585 confirmed cases and 38 probable cases from 28 May to 28 June. We note, however, that 63 imported cases were first removed for the data in.[24] This omission most likely resulted in an overestimation of the initial growth rate, by ignoring these imported cases that must have collectively played a significant role in the early local transmissions in the island nation. We note that the role of imported cases is problematic to quantitate when estimating transmissibility, as there are no 'local' source of infection for these imported cases. However, by discounting the imported cases, which in the case of New Zealand data accounts for more than 10% of total cases, one ignores the infections caused by the imported infective and hence inevitably overestimates the transmissibility of the remaining local cases.

There are several factors relating to imported cases that might impact the estimation of R, such as the timing and the size of the imported cases, the nature of the resulting local infections (e.g., household, community, nosocomial), and not the least of all the epidemiological characteristics of the disease under consideration. For example, a few imported cases at the early stages that set off a fast-spreading disease locally (e.g., pandemic influenza) would have a decidedly different effect when compared to the situation with imported cases scattered over a long period of time for a less transmissible disease with no apparent asymptomatic infections such as SARS, unless there are very fast-developing local clusters of infections or nosocomial spread, as in the 2003 SARS outbreak. A study on pH1N1 epidemic in Victoria, Australia, indicates that, by using methods designed to account for the undetected transmission caused by unidentified imported cases, the mean estimate for R reduces dramatically from 2·4 to 1·6.[26]

The reproduction number obtained for Brazil is only slightly higher than other southern hemisphere countries studied (see Figure 3), but with a much larger confidence interval. In the cases of Argentina and Brazil where both 1-wave and 2-wave Richards models fit the cumulative case data, R is always larger in the first phase in May to June, perhaps indicative of the initial severity or lack of immunity/intervention during early stages of a novel virus outbreak. We note that higher R for earlier data was also observed in,[22] after correction for ascertainment bias.

It is particularly interesting to note that for countries such as Argentina, Chile, New Zealand, and Australia, where multiple estimates were obtained from distinct epidemic data (case, hospitalization, and deaths), the estimates of R are highly comparable. Therefore, in events where the disease epidemic curve is not readily available or does not converge (as in the case of Chile), the hospitalization and deaths data, while not necessarily accurate for detecting the

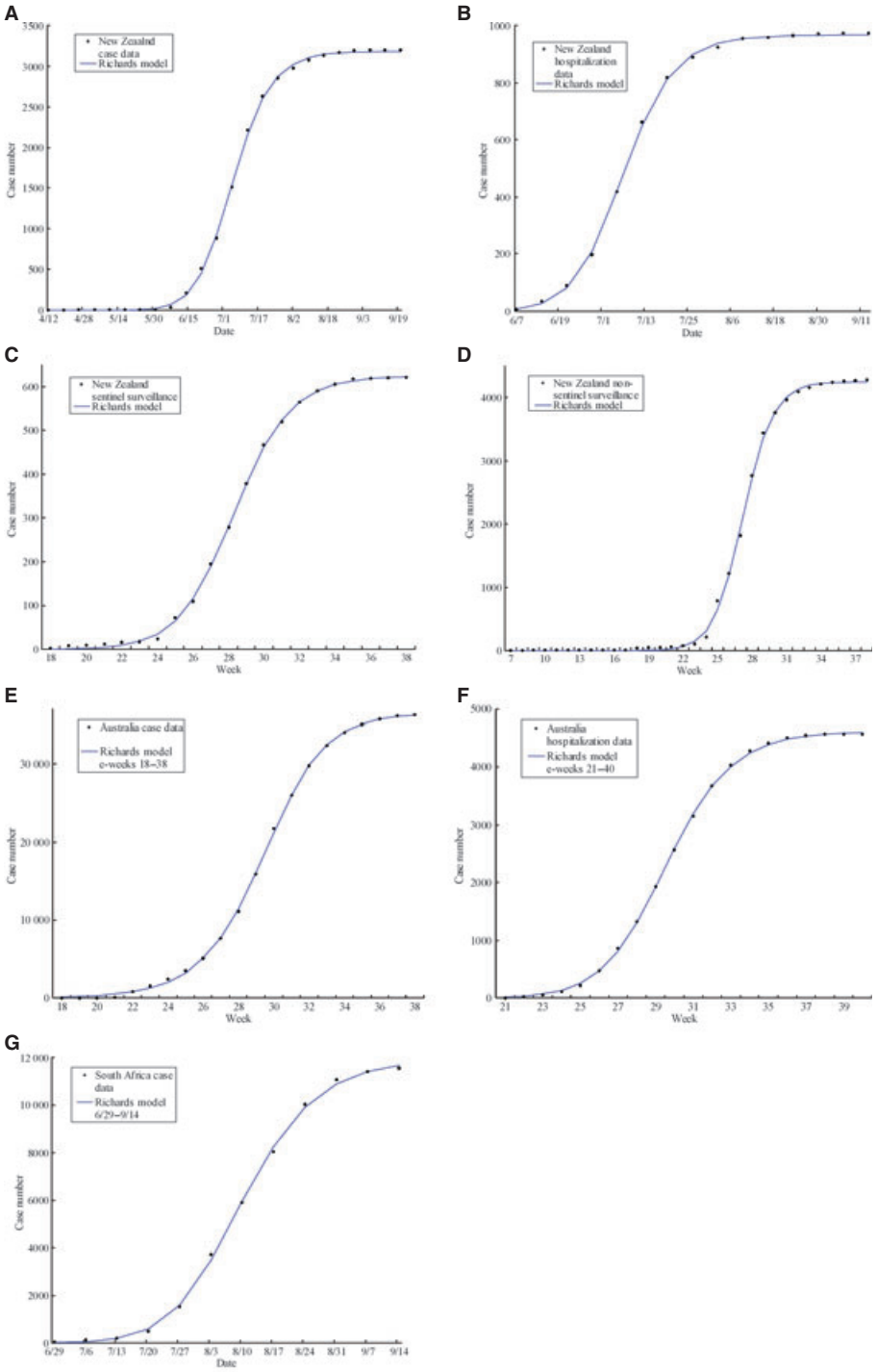

Figure 2. Theoretical curves obtained from 1-wave Richards model and 2009 H1N1 cumulative data: (2A) New Zealand weekly cumulative pH1N1 confirmed data by reporting week (week ending on 4/12–9/20); (2B) New Zealand weekly cumulative hospitalized cases by earliest reporting week (Week ending on 6/7–9/13); (2C) New Zealand weekly cumulative sentinel surveillance data (June 14–September 20); (2D) New Zealand weekly cumulative non-sentinel surveillance data (May 3–September 20); (2E) Australia weekly cumulative confirmed case data by onset week of e-weeks 18–38; (2F) Australia weekly cumulative hospitalization case data by onset week of e-weeks 21–40; (2G) South Africa daily cumulative confirmed case data by reporting week of weeks ending 7/5–9/20.

Table 6. Estimation results using weekly pH1N1 confirmed and hospitalized cases by reporting week in Australia with the 1-wave Richards model. Turning point t_i denotes the number of weeks after the beginning of the wave of outbreak. The actual case number is 36214 confirmed cases, 4573 for the hospitalizations

Data	E-weeks	Turning point t_i (95% C.I.)	Growth rate r (95% C.I.)	Case number K (95% C.I.)	R (95% C.I.)
Confirmed case	18–38	11·62 (e-week 30) (11·24, 12·00)	0·63 (0·57, 0·68)	36336 (35979, 36693)	1·19 (1·11, 1·26)
Hospitalization	21–40	8·40 (e-week 30) (7·87, 8·94)	0·53 (0·50, 0·57)	4621 (4588, 4654)	1·16 (1·09, 1·22)

Table 7. Estimation results using weekly pH1N1 confirmed cases by reporting week in South Africa with the 1-wave Richards model. Turning point t_i denotes the number of weeks after the beginning of the wave of outbreak. The actual case number is 11546

Time period	Turning point t_i (95% CI)	Growth rate r (95% CI)	Max case number K (95% CI)	R (95% CI)
Week ending on 7/5–9/20	5·76* (4·08, 7·44)	0·73 (0·55, 0·91)	11943 (11495, 12391)	1·22 (1·11, 1·33)

*The week ending on 8/16.

Table 8. Estimates of effective reproduction number R for Argentina data using estimates of T obtained from pH1N1 data of: US with (a) T = (2·6, 3·2)[19] and (b) T = 2·5[20]; (c) Netherlands: T = 2·7 (SD = 1·1)[21]; (d) Japan: T = 2·83 (Variance = 1·26) [Nishiura, personal communications]; (e) Mexico: T = 1·91 (95% CI: 1·30–2·71).[18]

Time period	Estimates of R				
	(a)	(b)	(c)	(d)	(e)
(A) Estimates of R using daily confirmed pH1N1 case data by onset date in Argentina with 1-wave and 2-wave Richards models					
1-wave (5/19–8/23)	1·69 (1·57, 1·81)	1·57 (1·51, 1·64)	1·63 (0·99, 2·27)	1·67 (1·00, 2·34)	1·41 (1·23, 1·60)
2-wave (5/19–6/4)	2·53 (0·66, 4·39)	2·22 (0·82, 3·63)	2·37 (0·07, 4·67)	2·47 (0*, 4·95)	1·84 (0·86, 2·82)
2-wave (6/4–8/23)	1·55 (1·47, 1·64)	1·46 (1·42, 1·50)	1·50 (1·01, 2·00)	1·53 (1·02, 2·05)	1·34 (1·19, 1·48)
(B) Estimates of R using daily sever respiratory infection (SRI) hospitalization data and pH1N1 death data in Argentina fitting with the 1-wave Richards model					
Hospitalization (6/1–7/25)	1·43 (1·37, 1·50)	1·36 (1·34, 1·39)	1·40 (1·02, 1·77)	1·42 (1·03, 1·81)	1·27 (1·16, 1·38)
Death (6/12–8/20)	1·45 (1·39, 1·51)	1·38 (1·37, 1·39)	1·42 (1·02, 1·81)	1·44 (1·03, 1·85)	1·28 (1·16, 1·39)

turning points or estimating the final outbreak size, can be used as surrogate data to rapidly estimate the reproduction number R of the outbreak.

Turning point

For Argentina and Brazil, two earlier turning points were detected through the 2-wave model, perhaps because of stochastic variations of early data or other factors such as changing case definition and level of surveillance/testing. However, the third turning point of the respective 2-wave models is in agreement with the single turning point of the respective 1-wave models, both detect e-week 31 in the case of Brazil and are separated by merely 2 days (June 24 and June 26) for Argentina, thus indicating that the detection of the most important turning point of the outbreak is robust.

Among the South American countries, the downturn turning point of the outbreak occurred earlier in Argentina and Chile in June, while Brazil did not experience its downtown until late July. New Zealand (early July) had its turning point slightly ahead of Australia (late July). For South Africa the outbreak did not turn for the better until mid-August.

Moreover, in countries where multiple epidemic data (cases, hospitalizations, and deaths) are available for model fit, the resulting turning points for reporting of cases, hospitalizations, and deaths always follow the proper chrono-

Table 9. Estimates of effective reproduction number *R* for New Zealand data using estimates of *T* obtained from pH1N1 data of: US with (a) *T* = (2·6, 3·2)[19] and (b) *T* = 2·5[20]; (c) Netherlands: *T* = 2·7 (SD = 1·1)[21]; (d) Japan: *T* = 2·83 (Variance = 1·26) [Nishiura, personal communications]; (e) Mexico: *T* = 1·91 (95% CI: 1·30–2·71)[18]

Data	Estimates of *R*				
	(a)	(b)	(c)	(d)	(e)
Confirmed case	1·04 (1·01, 1·08)	1·29 (1·26, 1·33)	1·32 (1·02, 1·62)	1·34 (1·03, 1·64)	1·23 (1·13, 1·33)
Hospitalization	1·06 (1·01, 1·10)	1·39 (1·33, 1·44)	1·43 (1·02, 1·83)	1·45 (1·03, 1·87)	1·29 (1·16, 1·41)
Sentinel surveillance	1·04 (1·01, 1·06)	1·24 (1·21, 1·27)	1·26 (1·03, 1·50)	1·28 (1·03, 1·52)	1·18 (1·10, 1·25)
Non-sentinel surveillance	1·04 (1·01, 1·08)	1·30 (1·25, 1·34)	1·33 (1·02, 1·63)	1·34 (1·03, 1·66)	1·22 (1·13, 1·31)

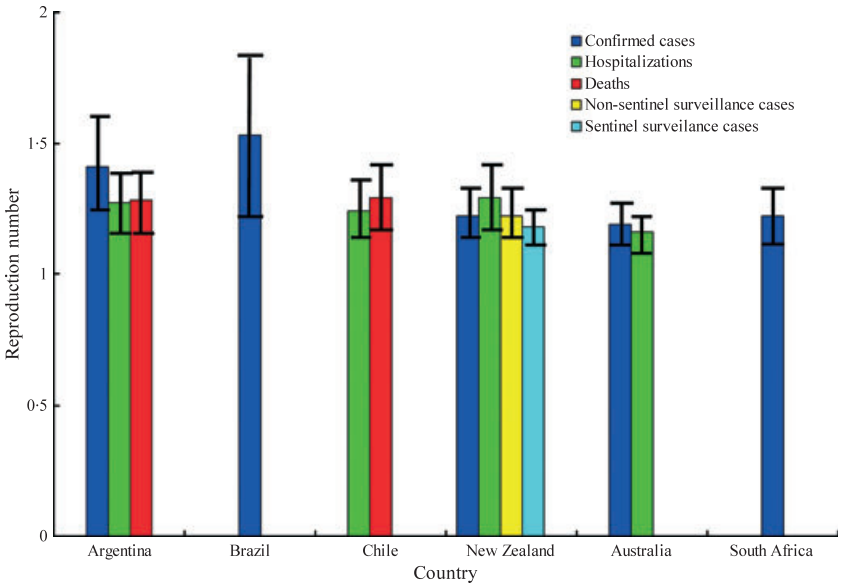

Figure 3. Reproduction numbers and their 95% confidence intervals (CI) for pandemic influenza A (H1N1) outbreaks in 6 southern hemisphere countries during the 2009 winter season in the southern hemisphere.

Table 10. Turning points for reporting of confirmed cases, hospitalizations, and deaths in Argentina, Chile, New Zealand, and Australia

Data	Country			
	Argentina	Chile	New Zealand	Australia
Confirmed cases	June 26	–	Week ending 7/5	7/19–7/25 (e-week 30)
Hospitalizations	June 28	6/21–6/27 (e-week 26)	Week ending 7/12	7/19–7/25
Deaths	July 1	July 11	–	–

logical order of disease progression (Table 10 and Figure 4), including that of Australia where the turning points for reporting of cases and hospitalizations fall on the same e-week. This gives further credence to the detection of turning points of an outbreak, not only for disease incidence but also for the temporal changes in disease progression and treatment of the infected individuals.

We note that in general the turning points of an outbreak correspond to peaks and valleys in the epidemic curve. However, as a result of stochastic variations, multiple spikes often appear around the peaks. Moreover, some temporary deceleration or acceleration in the cumulative rate might not be related to a declining epidemic. The Richards model has the advantage of isolating a small range of time period during which the turning points (up turns and down turns) may have occurred.[13–16, 25] We also note that the estimates for the outbreak sizes, *K*, also closely approximate the actual case numbers for the periods of

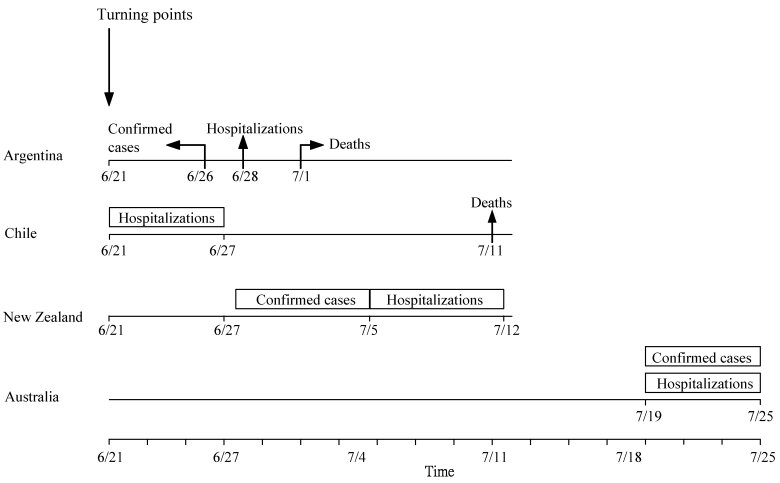

Figure 4. Chronological timelines of the turning points for cases, hospitalizations, or deaths during the summer pH1N1 epidemics in Argentina, Chile, Australia, and New Zealand. Note that the turning point is by date for Argentina and by week for the other three countries.

outbreak being fitted (provided in the table legends), which is not surprising given the reasonable model fit obtained.

The limitations of the Richards model have been thoroughly discussed previously in,[14, 16] and hence are not repeated here. In addition to existing pre-immunity, estimates of *R* may also be influenced by factors such as social mixing patterns, access to medical care, and level of intervention measures in each country. To address this issue, model specific for each country is required to account for the social mixing and healthcare infrastructure of each country, as well as any specific interventions that were implemented, but is beyond the scope of this work.

Numerous sophisticated models have been proposed (e.g., 27–30) that give time-dependent reproduction number *R*, which could change with time owing to interventions and/or susceptible depletion but requires more detailed and high-quality data. Nevertheless, the Richards model provides a swift and viable method to quick estimate of *R* as well as identifying the important turning points of the outbreak, with a minimal requirement of epidemic data that are typically available to the public. It is interesting to note that, for Argentina, the hospitalization data for confirmed pH1N1 cases are not available on the web; therefore, we used the hospitalization data for severe respiratory infections, which include but are not limited to the confirmed pH1N1 cases. However, the resulting estimate for reproduction number is surprisingly similar to the estimates using the case data or the death data. Moreover, the estimated turning point for hospitalizations is also consistent with those of cases and deaths.

Most of the southern hemisphere countries studied are of substantial size, and thus the epidemic had different timings in different regions. For example, in Australia, the epidemic in Victoria was a full month ahead of some other states might well have impacted the epidemic in other states. In such cases, instead of using national totals, the detailed data for each region are needed to account for the regional heterogeneity. However, other factors such as the level of mobility between regions must then be considered, which would call for a complicated model with spatial elements, which is again beyond the scope of this study.

In summary, our results suggest that the winter pandemic A (H1N1) outbreak in the southern hemisphere, as indicated by its reproduction number, was not dissimilar to the earlier spring epidemics[23] or the fall/winter outbreaks in the northern hemisphere based on preliminary results of an ongoing study of the fall/winter outbreak in Taiwan using the same modeling approach. Therefore, the current strain, while circulating around the globe, has not become more severe or transmissible either in the southern or in the northern hemisphere, as some experts had cautioned. The results, which corroborate earlier findings that the 2009 pandemic had not been severe in the southern hemisphere,[31] will be useful for global preparedness planning of possible tertiary waves of pH1N1 infections in the fall/winter of both southern and northern hemispheres in 2010.

Acknowledgements

YHH is supported by grants (NSC 97-2314-B-039-013-MY3, NSC 97-2118-M-039-004, and CMU 97 323). The author is grateful to the reviewers for their insightful comments and suggestions, which significantly improved this manuscript.

References

1 Ginsberg M, Hopkins J, Maroufi A *et al.* Swine Influenza A (H1N1) Infection in Two Children – Southern California, March-April 2009. MMWR 2009; 58(15):400–402. Available at http://www.cdc.gov/mmwr/preview/mmwrhtml/mm5815a5.htm.

2 World Health Organization. Pandemic (H1N1) 2009 – update 88. 19 February 2010. http://www.who.int/csr/don/2010_02_19/en/index.html (Accessed 22 February 2010).

3 Lipsitch M, Riley S, Cauchemez S, Ghani AC, Ferguson NM. Managing and Reducing Uncertainty in an Emerging Influenza Pandemic. N Engl J Med 2009; 361:112–115.

4 Ministry of Health of Argentina. INFLUENZA PANDÉMICA (H1N1) 2009 REPÚBLICA ARGENTINA, INFORME SEMANA EPIDEMIOLÓGICA Nº 33. Available at http://www.msal.gov.ar/htm/Site/default.asp (Accessed 1 September 2009).

5 Ministry of Health of Chile. INFLUENZA PANDÉMICA (H1N1) 2009. Available at http://www.redsalud.gov.cl/minsalaudios/reporte26agosto.pdf (Accessed 29 September 2009).

6 Brazilian Ministry of Health. Informe Influenza, August 24, 2009. Available at http://portal.saude.gov.br/portal/arquivos/pdf/informe_influenza_se_33_24_08_2009.pdf (Accessed 1 September 2009).

7 Institute of Environmental Science and Research of New Zealand. New Zealand Influenza weekly update, 2009/35: August 24–30, 2009. Available at http://www.surv.esr.cri.nz/PDF_surveillance/Virology/FluWeekRpt/2009/FluWeekRpt200938.pdf (Accessed 29 September 2009).

8 Department of Health and Ageing of Australia. Influenza Surveillance Report No. 19, for the week ending 18 September 2009. Available at http://www.healthemergency.gov.au/internet/healthemergency/publishing.nsf/Content/D172E87918D1CE17CA25763E00823443/$File/ozflu-no19-2009.pdf (Accessed 29 September 2009).

9 The National Institute for Communicable Diseases (NICD) of South Africa. NICD Weekly Situation Report, 24 September, 2009. Available at http://www.nicd.ac.za/pubs/communique/2009/sitrep/NovelInfA_22_09_2009SitRep.pdf (Accessed 29 September 2009).

10 Richards FJ. A flexible growth function for empirical use. J Exp Bot 1959; 10:290–300.

11 Wallinga J, Lipsitch M. How generation intervals shape the relationship between growth rates and reproductive numbers. Proc Biol Sci 2007; 274:599–604.

12 Nishiura H, Chowell G, Heesterbeek H, Wallinga J. The ideal reporting interval for an epidemic to objectively interpret the epidemiological time course. J R Soc Interface 2010; 7(43):297–307.

13 Hsieh YH, Lee JY, Chang HL. SARS epidemiology. Emerg Infect Dis 2004; 10(6):1165–1167.

14 Hsieh YH, Cheng YS. Real-time forecast of multi-wave epidemic outbreaks. Emerg Infect Dis 2006; 12(1):122–127.

15 Hsieh YH. Richards Model: a simple procedure for real-time prediction of outbreak severity. in Ma Z, Wu J, Zhou Y, (eds): Modeling and Dynamics of Infectious Diseases. Series in Contemporary Applied Mathematics (CAM), Vol. 11, 2008.9, Beijing: Higher Education Press, 2008.

16 Hsieh YH, Chen CWS. Turning points, reproduction number, and impact of climatological events on multi-wave dengue outbreaks. Trop Med Int Health 2009; 16(4):1–11.

17 Mathews JD, Chesson JM, McCaw JM, McVernon J. Understanding influenza transmission, immunity and pandemic threats. Influenza Other Respi Viruses 2009; 3(4):143–149.

18 Fraser C, Donnelly CA, Cauchemez S *et al.* Pandemic potential of a strain of Influenza A (H1N1): early findings. Science 2009; 324(5934):1557–1561.

19 Yang Y, Sugimoto JD, Halloran ME *et al.* The transmissibility and control of pandemic influenza A (H1N1) virus. Science 2009; 326:729–733.

20 White LF, Wallinga J, Finelli L *et al.* Estimation of the reproductive number and the serial interval in early phase of the 2009 influenza A/H1N1 pandemic in the USA. Influenza Other Respi Viruses 2009; 3:267–276.

21 Hahné S, Donker T, Meijer A *et al.* Epidemiology and control of influenza A(H1N1)v in the Netherlands: the first 115 cases. Euro Surveill 2009; 14(27):19267.

22 Pourbohloul B, Ahued A, Davoudi B *et al.* Initial human transmission dynamics of the pandemic (H1N1) 2009 virus in North America. Influenza Other Respi Viruses 2009; 3(5):215–222.

23 Transmission dynamics and impact of pandemic infl uenza A (H1N1) 2009 virus. Wkly Epidemiol Rec 2009; 84(46):481–484.

24 Nishiura H, Wilson N, Baker MG. Estimating the reproduction number of the novel influenza A virus (H1N1) in a Southern Hemisphere setting: preliminary estimate in New Zealand. NZ Med J 2009; 122(1299):73–77.

25 Hsieh YH, Ma S. Intervention measures, turning point, and reproduction number for dengue, Singapore, 2005. Am J Trop Med Hyg 2009; 80:66–71.

26 McBryde ES, Bergeri I, van Gemert C *et al.* Early transmission characteristics of influenza A(H1N1)v in Australia: Victorian state, 16 May – 3 June 2009. Euro Surveill 2009; 14(42):19363.

27 Wallinga J, Teunis P. Different epidemic curves for severe acute respiratory syndrome reveal similar impacts of control measures. Am J Epidemiol 2004; 160:509–516.

28 Cauchemez S, Boëlle PY, Thomas G, Valleron AJ. Estimating in real time the efficacy of measures to control emerging communicable diseases. Am J Epidemiol 2006; 164(6):591–597.

29 Bettencourt LMA, Ribeiro RM. Real Time Bayesian estimation of the epidemic potential of emerging infectious diseases. PLoS ONE 2008; 3(5):e2185.

30 White LF, Pagano M. A likelihood-based method for real-time estimation of the serial interval and reproductive number of an epidemic. Stat Med 2008; 27(16):2999–3016.

31 Baker MG, Kelly H, Wilson N. Pandemic H1N1 influenza lessons from the southern hemisphere. Euro Surveill 2009; 14(42):19370. Available online: http://www.eurosurveillance.org/ViewArticle.aspx?ArticleId=19370.